

ORIGINAL ARTICLE

# Similarities and Differences of Early Pulmonary CT Features of Pneumonia Caused by SARS-CoV-2, SARS-CoV and MERS-CoV: Comparison Based on a Systemic Review

Xu Chen, Gang Zhang, Shuaiying Hao, Lin Bai\*, Jingjing Lu\*

Department of Radiology, Beijing United Family  
Hospital, Beijing 100015, China

**Key words:** computer tomography; pneumonia, viral; COVID-19; severe acute respiratory syndrome coronavirus; Middle East respiratory syndrome coronavirus; severe acute respiratory syndrome coronavirus 2

**Objective** To compare the similarities and differences of early CT manifestations of three types of viral pneumonia induced by SARS-CoV-2 (COVID-19), SARS-CoV (SARS) and MERS-CoV (MERS) using a systemic review.

**Methods** Electronic database were searched to identify all original articles and case reports presenting chest CT features for adult patients with COVID-19, SARS and MERS pneumonia respectively. Quality of literature and completeness of presented data were evaluated by consensus reached by three radiologists. Vote-counting method was employed to include cases of each group. Data of patients' manifestations in early chest CT including lesion patterns, distribution of lesions and specific imaging signs for the three groups were extracted and recorded. Data were compared and analyzed using SPSS 22.0.

**Results** A total of 24 studies were included, composing of 10 studies of COVID-19, 5 studies of MERS and 9 studies of SARS. The included CT exams were 147, 40, and 122 respectively. For the early CT features of the 3 pneumonias, the basic lesion pattern with respect to "mixed ground glass opacity (GGO) and consolidation, GGO mainly, or consolidation mainly" was similar among the 3 groups ( $\chi^2 = 7.966, P > 0.05$ ). There were no significant differences on the lesion distribution ( $\chi^2 = 13.053, P > 0.05$ ) and predominate involvement of the subpleural area of bilateral lower lobes ( $\chi^2 = 4.809, P > 0.05$ ) among the 3 groups. The lesions appeared more focal in COVID-19 pneumonia at early phase ( $\chi^2 = 23.509, P < 0.05$ ). The proportions of crazy-paving pattern ( $\chi^2 = 23.037, P < 0.001$ ), organizing pneumonia pattern ( $P < 0.05$ ) and pleural effusions ( $P < 0.001$ ) in COVID-19 pneumonia were significantly lower

than the other two. Although rarely shown in the early CT findings of all three viral pneumonias, the fibrotic changes were more frequent in SARS than COVID-19 and MERS ( $\chi^2 = 6.275$ ,  $P < 0.05$ ). For other imaging signs, only the MERS pneumonia demonstrated tree-in-buds, cavitation, and its incidence rate of interlobular or intralobular septal thickening presented significantly increased as compared to the other two pneumonia ( $\chi^2 = 22.412$ ,  $P < 0.05$ ). No pneumothorax, pneumomediastinum and lymphadenopathy was present for each group.

**Conclusions** Imaging findings on early stage of these three coronavirus pneumonias showed similar basic lesion patterns, including GGO and consolidation, bilateral distribution, and predominant involvement of the subpleural area and the lower lobes. Early signs of COVID-19 pneumonia showed less severity of inflammation. Early fibrotic changes appeared in SARS only. MERS had more severe inflammatory changes including cavitation and pleural effusion. The differences may indicate the specific pathophysiological processes for each coronavirus pneumonia.

**S**INCE late December, 2019, an outbreak of a novel coronavirus disease (COVID-19; previously known as 2019-nCoV)<sup>[1, 2]</sup> was reported in Wuhan, China, which has subsequently affected 26 countries worldwide.<sup>[2]</sup> As of now, although outbreak of the novel coronavirus pneumonia is not yet fully under control, many researches about the novel coronavirus and its pathogenic mechanism have been published continuously, and related clinical and therapeutical knowledge is updated on a weekly basis.

Medical imaging played an important role during the course of the pneumonia diagnosis and follow-up. CT has been an important imaging modality in assisting in the diagnosis and management of patients with COVID-19 pneumonia, and reports on the radiological appearances of COVID-19 pneumonia are emerging. Because chest radiography is not sensitive for the early detection of subtle changes such as ground-glass opacity (GGO) and may demonstrate normal findings in early stage of infection, chest CT functions more effectively in early detection of COVID-19 pneumonia. Currently, CT is of unique importance as it is the main tool for screening, primary diagnosis, and evaluation of disease severity.<sup>[3]</sup> Dozens of imaging papers published revealed some relatively characteristic manifestations on chest CT images at early stage.<sup>[4-14]</sup>

The virus is formally named severe acute respiratory syndrome coronavirus 2 (SARS-CoV-2). The genetic sequence analysis revealed that the SARS-CoV-2 belongs to the  $\beta$ -coronavirus genus, with a 79.0% nucleotide identity to severe acute respiratory syndrome coronavirus (SARS-CoV) and 51.8% identity to Middle East respiratory syndrome coronavirus (MERS-CoV).<sup>[15]</sup> Latest histopathological report<sup>[16, 17]</sup> presented that there are some similar pathological basis between the

COVID-19 pneumonia and other two types of pneumonias induced by SARS-CoV and MERS-CoV. Past imaging studies also revealed a certain similar radiological appearance both for the SARS-CoV and the MERS-CoV pneumonia.<sup>[18]</sup> However, there is no comparison study reported on CT imaging features among these three coronavirus pneumonias on its early phase, to the best of our knowledge.

In this study, we were trying to reveal similarities and differences of the early CT features among the three types of viral pneumonias infected by SARS-CoV-2, SARS-CoV and MERS-CoV respectively through a systemic review.

## MATERIALS AND METHODS

### Search strategy and article inclusion

We included all original articles and case reports presenting viral pneumonia induced by SARS-CoV-2, SARS-CoV and MERS-CoV. Relevant papers were identified by computerized searches of PUBMED, Web of Science and WANGFANG till February 24th 2020, and using different combination of search words as follows: CT, imaging, radiologic, pneumonia, SARS, MERS, and COVID-19. We also used the bibliography of retrieved articles to further identify relevant studies. The inclusion criteria were: (1) observational studies or case reports related to CT imaging features of pneumonia infected by the SARS-CoV-2, SARS-CoV and MERS-CoV; (2) pathology or cytology examinations or mechanism were used as the gold standard of diagnosis. Exclusion criteria were: (1) duplicate publications or data; (2) publications related to chest X ray or radiograph only; (3) publication related to late follow up or convalescence; (4) publication in languages other than English or Chinese; and (5) insufficient data available in the original publication.

### Data collection and recording

Simple vote-counting method was employed to record the different radiological features for each included observational study. The CT exam and imaging finding data were collected from the included articles and recorded by three authors using same criteria.

The recorded data included: (1) Age, gender, system of onset, availability of the early chest CT (For each patient, we defined the early CT scans as which obtained within 1 week after onset of symptoms). (2) Extraction and classification of imaging pattern and features, including distribution of lesions and the features as followed: GGO, consolidation, nodular lesion, inter- or intra-lobular septal thickening, fibrotic changes, tree-in-bud sign, crazy paving pattern, cavitation, organizing pneumonia, pneumomediastinum, pneumothorax, lymphadenopathy, and pleural effusion.

Imaging pattern and features were defined as follows with reference to Ref 19-21.<sup>[19-21]</sup> The geographic distribution of lesions was defined as: unilateral or bilateral, focal or multifocal or extensive, predilection to lower lobes or no predilection to lower lobe. The transverse distribution of the abnormalities was categorized as central (i.e., peribronchovascular), peripheral (i.e., subpleural), or no transverse predilection. Nodular opacities were defined as focal round opacities. Fibrotic changes included traction bronchiectasis, reticulation, irregular linear opacities, and stellate or subpleural bands. Pleural effusion, other complications such as pneumothorax and pneumomediastinum, and other coexisting abnormalities (e.g., emphysema bullae) if any, were also recorded.

Disagreements were resolved by discussion among all authors during the process of data abstraction and classification. If the parameter could not be counted for certain cases included in the study, the parameter was defined as "not accessible" and the certain cases were excluded from the calculation of percentage.

### Statistical analysis

Qualitative variables were presented as frequency and percentage. Presence or absence of other CT parameters (GGO, consolidation, cavitation, pleural effusion, tree-in-bud, crazy paving, and inter- or intra-lobular septal thickening) were compared between the two groups using a *Chi-square* test for categorical data. A *P* value (two-tailed) less than 0.05 was considered statistically significant. SPSS software (22.0, IBM) was

used for statistical analysis.

## RESULTS

### General features of the included studies

A total of 90 publications were initially identified, 88 of which were written in English and 2 in Chinese. After evaluation using inclusion and exclusion criteria, a total of 24 publications were included in the study (**Figure 1**).<sup>[3-13, 19, 21-32]</sup> The characteristics of the 24 studies are listed in **Table 1**. The basic results of the pooled study and CT availability information are listed in **Table 2**.

### Basic lesion pattern and imaging features on early phase chest CT of COVID-19, MERS and SARS pneumonia

For the early CT of the three coronavirus pneumonias, the basic lesion pattern with respect to "mixed GGO and consolidation, GGO mainly, or consolidation mainly" was similar among the 3 groups ( $\chi^2=7.966$ ,  $P=0.093$ ). There were no significant differences on the lesion distribution ( $\chi^2=13.053$ ,  $P>0.05$ ) and predominate involvement of the subpleural area of bilateral lower lobes ( $\chi^2=4.809$ ,  $P>0.05$ ) among the three groups. The lesion appeared more focal in COVID-19 pneumonia at early phase ( $\chi^2=23.509$ ,  $P<0.05$ ). The proportions of crazy-paving pattern ( $\chi^2=23.037$ ,  $P<0.001$ ), organizing pneumonia pattern ( $P<0.05$ ) and pleural effusions ( $P<0.001$ ) in COVID-19 pneumonia were significantly lower than the other two. The incidence rate of interlobular or intralobular septal thickening presented in COVID-19 significantly increased as

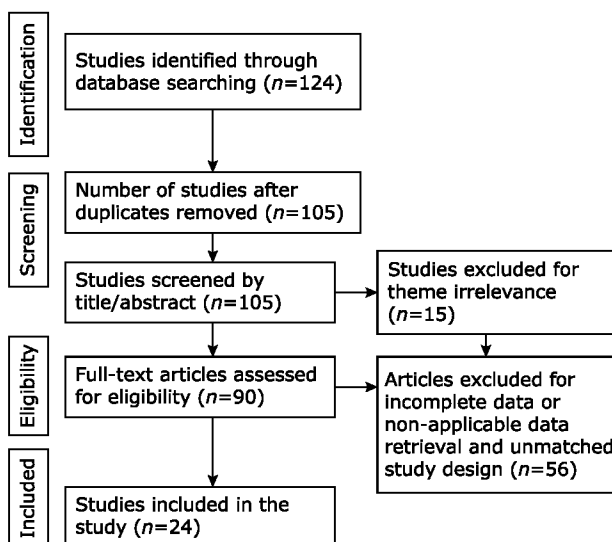


**Figure 1.** Flow diagram of study selection.

**Table 1.** Main characteristics of the included studies

References	Year	Country	Publication type	Sample size (n)
<b>COVID-19</b>				
Xie <i>et al.</i> <sup>[4]</sup>	2020	China	Case reports	5
Lei <i>et al.</i> <sup>[5]</sup>	2020	China	Case report	11
Fang <i>et al.</i> <sup>[6]</sup>	2020	China	Case report	2
Shi <i>et al.</i> <sup>[7]</sup>	2020	China	Case report	1
Pan <i>et al.</i> <sup>[8]</sup>	2020	China	Article	52
Lin <i>et al.</i> <sup>[9]</sup>	2020	China	Case report	2
Fang <i>et al.</i> <sup>[10]</sup>	2020	China	Article	51
Pan <i>et al.</i> <sup>[11]</sup>	2020	China	Article	21
Duan <i>et al.</i> <sup>[12]</sup>	2020	China	Case report	1
Fang <i>et al.</i> <sup>[13]</sup>	2020	China	Case report	1
<b>MERS</b>				
Ajlan <i>et al.</i> <sup>[3]</sup>	2015	Saudi Arabia	Case reports	7
Das <i>et al.</i> <sup>[22]</sup>	2016	Saudi Arabia	Article	15
Choi <i>et al.</i> <sup>[23]</sup>	2016	Korea	Case report	1
Hamimi <i>et al.</i> <sup>[24]</sup>	2015	Saudi Arabia	Article	8
Das <i>et al.</i> <sup>[25]</sup>	2017	Saudi Arabia	Article	9
<b>SARS</b>				
Zhao <i>et al.</i> <sup>[26]</sup>	2003	China	Article	8
Goh <i>et al.</i> <sup>[27]</sup>	2003	Singapore	Case report	1
Nicolaou <i>et al.</i> <sup>[28]</sup>	2003	Canada	Case report	1
Wang <i>et al.</i> <sup>[29]</sup>	2003	China	Article	112
Müller <i>et al.</i> <sup>[30]</sup>	2003	Canada	Article	12
Zeng <i>et al.</i> <sup>[31]</sup>	2003	China	Article	61
Ooi <i>et al.</i> <sup>[21]</sup>	2003	Hong Kong	Article	30
Chan <i>et al.</i> <sup>[19]</sup>	2004	Hong Kong	Article	27
Müller <i>et al.</i> <sup>[32]</sup>	2004	Canada	Article	29

COVID-19: severe acute respiratory syndrome coronavirus 2; MERS: Middle East respiratory syndrome coronavirus; SARS: severe acute respiratory syndrome coronavirus.

compared to SARS and MERS pneumonias ( $\chi^2 = 22.412$ ,  $P < 0.05$ ). Although rarely shown in the early CT findings from all three viral pneumonias, the fibrotic changes were more frequent in SARS than COVID-19 and MERS ( $\chi^2 = 6.275$ ,  $P < 0.05$ ). More detailed results are listed in **Table 3**.

**Table 2.** Basic results of the pooled study and CT availability information

Disease category	Number of included studies (n)	Number of included patients (n)	Mean age (yrs)	Early phase CT* (n)
COVID-19	10	147	44.8	147
MERS	5	40	44.8	37
SARS	9	122	40.4	85

\*Early phase CT indicated CT exams undertaken within the 1st week of symptom onset.

For other imaging signs, only the MERS-CoV induced pneumonia demonstrated tree-in-buds ( $n=5$ ), cavitation ( $n=4$ ). No pneumothorax, pneumomediastinum and lymphadenopathy was present for each group.

## DISCUSSION

In this study, we designed the systemic review of literatures and found similarities and differences of the early CT image features in three types of pneumonias caused by SARS-CoV-2 (COVID-19), SARS-CoV (SARS) and MERS-CoV (MERS) respectively.

The early use of chest CT as a screening tool for patients with suspected COVID-19 has been employed in certain area of high prevalence. Early pulmonary CT not only decrease missed diagnosis which might occurred on chest radiograph, but can also help to identify those patients with COVID-19 who had initial negative real time reverse-transcription polymerase chain reaction (RT-PCR) results.<sup>[4]</sup> The medical team including pulmonologists and radiologists in Wuhan strongly recommends CT scan as the main diagnostic and screening basis for COVID-19. The "Diagnosis and Treatment Scheme for Coronavirus Disease" specifically formulated clinical diagnosis standards for patients in Hubei Province, and defined suspected cases with pneumonia imaging manifestations as "clinical diagnostic cases", which reduced the risk of further spread.<sup>[33]</sup>

Based on our current review, the basic imaging features on early CT of these three types of pneumonias caused by SARS-CoV-2, SARS-CoV and MERS-CoV were diffuse airspace opacities which present as GGO, consolidation or mixed GGO and consolidation. The airspace opacities were often seen in subpleural or peripheral area of bilateral lobes, starting from the lower lobes. Such imaging features are pathogenomic for coronavirus pneumonia in certain scenario.<sup>[14, 18]</sup> Abnormal lung CT findings can be present even in asymptomatic patients, and lesions can rapidly evolve into a diffuse GGO predominance or consolidation pattern within 1-3 weeks after onset of symptoms, peaking at around 2 weeks after onset.<sup>[14]</sup>

**Table 3.** Comparison of imaging features and patterns of early phase CT for COVID-19, MERS and SARS [n (%)]

Items	COVID-19	MERS	SARS	$\chi^2$	P
Total number of early phase CT	147	37	85		
GGO consolidation pattern				7.966	0.093
Mixed GGO&Consolidation	41(27.9)	10(27.0)	23(27.1)		
GGO mainly	89(60.5)	16(43.2)	49(57.6)		
Consolidation mainly	17(11.6)	11(29.7)	13(15.3)		
Laterality				13.053	0.316
Bilaterality	98(66.7)	25(67.6)	39(78.0)		
Unilaterality	49(33.3)	12(32.4)	11(22.0)		
Not accessible* (n)	0	0	35		
More severe in the lower lobes				4.809	0.535
Yes	60(74.7)	27(73.0)	11(61.1)		
No	21(25.9)	10(27.0)	7(38.9)		
Not accessible* (n)	66	0	67		
Geographic distribution				23.509	<0.05
Focal	45(40.5)	6(16.2)	18(42.8)		
Multifocal	66(59.5)	20(54.0)	16(38.1)		
Extensive	0	11(29.7)	8(19.1)		
Not accessible* (n)	36	0	43		
Transverse distribution				13.053	<0.001
Central	15(17.8)	8(21.6)	3(4.7)		COVID-19 vs. SARS, P<0.001
Peripheral	55(65.4)	17(45.9)	28(44.4)		COVID-19 vs. MERS, P=0.09
No predilection	14(16.7)	12(32.4)	32(50.8)		SARS vs. MERS, P=0.02
Not accessible* (n)	63	0	22		
Nodular lesion	0	4(10.8)	14(15.7)		<0.001
Septal thickening	17(11.6)	16(43.2)	12(13.5)	22.412	<0.001
Fibrotic changes	2(1.4)	2(5.4)	7(7.9)	6.275	<0.05
Tree-in-bud	0	5(13.5)	0		<0.05
Cavitation	0	4(10.8)	0		<0.05
Crazy paving pattern	10(6.8)	10(27.0)	26(29.2)	23.037	<0.001
Organizing pneumonia pattern	1(0.7)	4(10.8)	7(7.9)		<0.05
Pleural effusion	0(0)	21(56.8)	12(13.5)		<0.001

GGO: ground-glass opacity. Percentage comparison among three groups or between two groups was performed using *Chi-Square* test. *P* value represents the comparison among the three groups unless specified.

\*"Not accessible" means the parameter cannot be counted for certain cases included in the study.

The pathological basis of the airspace opacities is diffuse alveolar damages including intra-alveolar edema, fibrin, and variable cellular infiltrates with a hyaline membrane, which is commonly associated with the histological features in the early phase of pulmonary SARS-CoV and MERS-CoV infection, even COVID-19 infection.<sup>[16, 17, 34]</sup> The similarity of lesion pattern could be supported by the information that the SARS-CoV-2 belongs to the  $\beta$ -coronavirus genus. Besides, it could be infer that the subpleural or peripheral distribution

of bilateral lower lobes as predilection site, often seen in many viral pulmonary diseases, was probably due to the size of pathogenic microorganism particles and its mechanism of attacking the alveolar epithelium. On the other hand, differences were also noted among the three coronavirus pneumonia with regards to other radiological features including septal thickening, tree-in-bud, cavitation, crazy-paving pattern, organizing pneumonia pattern and pleural effusion. Early signs of COVID-19 showed less severity of inflammation. This

imaging findings parallel the clinical progress pattern of COVID-19 patients who showed mild respiratory syndromes and less symptoms involving the other systems, such as intestinal system.<sup>[14, 35]</sup> But at the same time, it is noteworthy that the early clinical application of chest CT for COVID-19 patients. Of the 53 patients in the study of Li *et al*, positive CT findings diagnostic of viral pneumonia were available before a positive laboratory test result in 37 (69.8%) patients. The diagnosis of viral pneumonia based on CT was available 3.0 days earlier than that based on nucleic acid test results.<sup>[36]</sup> The reason may partially lie on the wide availability and recognition of CT as a useful diagnostic tool in current era.

Early fibrotic changes appear in SARS only. Fibrotic changes were frequently described in later or recovery phase CT for SARS pneumonia.<sup>[37, 38]</sup> Fibrotic changes reflects the parenchymal scarring of the inflamed lung tissue and probably relates to injured respiratory function.<sup>[39]</sup> Evidence is still lacking regarding this perspective for COVID-19 patients.

MERS had more severe inflammatory changes including the septal thickening, cavitation and pleural effusion. A few studies indicated that the pathological features of MERS-CoV infection include pulmonary edema, type II pneumocyte hyperplasia and interstitial pneumonia except from exudative diffuse alveolar damage with hyaline membranes. Bronchial submucosal necrosis was also observed. These lesions comprise the pathologic basis for the respiratory failure and radiologic abnormalities of MERS-CoV infection.<sup>[16, 40]</sup> It is not difficult to explain that the inflammatory process in MERS infection was more severe than COVID-19 and SARS.

The innovative point of our study is that we firstly reported the comparison of radiological features for the three coronavirus pneumonias on basis of a systematic literature review and analysis. COVID-19 still needs to be studied deeply in case it becomes a global health threat. In clinical practice, we already found early phase CT is a reliable and feasible test which provides differential diagnosis quickly when combined with epidemiological, clinical and laboratory results for suspected patients. That is especially the case when real-time reverse transcription polymerase chain reaction is slow and not accessible widely.

We acknowledge three main limitations of our study. First, our study is of its retrospective nature and basis of literature review, some included cohort was small and sequential CT study was not performed;

hence, we were not able to compare both the early and late CT findings in patients of all the three groups. Only early phase CT was included in our study, but at the same time, we believe the early CT signs are more pathognomonic as compared with progressive phase CT and even the severe phase as adult respiratory distress syndrome. Secondly, because of the year gap between the included studies, the technologies and intervention were evolving. There would be diverse uncontrolled factors affecting the collection and the comparison in the study and some bias is unavoidable. Thirdly, the literature on clinical and chest CT findings of COVID-19 is still expanding very quickly. It is not easily feasible to get the most updated literatures on COVID-19 in this study. At the same time, we believe the case number included for COVID-19 is appropriate since it is balanced as compared with the case numbers included for MERS and SARS (147 vs. 37 & 85 cases respectively) in this systemic review using comparative study design.

In summary, imaging findings on early stage of these three coronavirus pneumonias showed similar basic lesion pattern, including GGO and consolidation, bilateral distribution, and predominate involvement of the subpleural area and the lower lobes. Early signs of COVID-19 showed less severity of inflammation. Early fibrotic changes appeared in SARS pneumonia only. MERS had more severe inflammatory changes including cavitation and pleural effusion. The differences may indicate the specific pathophysiological processes for each coronavirus pneumonia. Further investigation is warranted to elucidate the pathophysiological basis for the difference and the correlation with the clinical disease progress.

#### **Acknowledgements**

*We thank Xiaoping Liu and Professor Lihua Mao from School of Psychological and Cognitive Sciences, Peking University for the helpful instructions in data analysis. We thank Dr. Mengyan Sun from Beijing Chest Hospital, Beijing Medical University for the kind help of literature searching.*

#### **Conflict of Interests Statement**

*The authors have no conflict of interests to disclose.*

#### **REFERENCES**

1. Wu F, Zhao S, Yu B, et al. A new coronavirus associ-

- ated with human respiratory disease in China. *Nature* 2020; 579(7798):265-9. doi: 10.1038/s41586-020-2008-3.
2. Huang C, Wang Y, Li X, et al. Clinical features of patients infected with 2019 novel coronavirus in Wuhan, China. *Lancet* 2020; 395(10223):497-506. doi: 10.1016/S0140-6736(20)30183-5.
  3. Ajlan AM. Reply to "Chest CT findings in MERS". *AJR Am J Roentgenol* 2015; 204(1):W112. doi: 10.2214/AJR.14.13367.
  4. Xie X, Zhong Z, Zhao W, et al. Chest CT for typical 2019-nCoV pneumonia: relationship to negative RT-PCR testing. *Radiology* 2020; 296(2):E41-E5. doi: 10.1148/radiol.20200343.
  5. Lei J, Li J, Li X, et al. CT imaging of the 2019 novel coronavirus (2019-nCoV) pneumonia. *Radiology* 2020; 295(1):18. doi: 10.1148/radiol.20200236.
  6. Fang Y, Zhang H, Xu Y, et al. CT manifestations of two cases of 2019 novel coronavirus (2019-nCoV) pneumonia. *Radiology* 2020; 295(1):208-9. doi: 10.1148/radiol.20200280.
  7. Shi H, Han X, Zheng C. Evolution of CT manifestations in a patient recovered from 2019 novel coronavirus (2019-nCoV) pneumonia in Wuhan, China. *Radiology* 2020; 295(1):20. doi: 10.1148/radiol.20200269.
  8. Pan Y, Guan H, Zhou S, et al. Initial CT findings and temporal changes in patients with the novel coronavirus pneumonia (2019-nCoV): a study of 63 patients in Wuhan, China. *Eur Radiol* 2020; 30(6):3306-9. doi: 10.1007/s00330-020-06731-x.
  9. Lin X, Gong Z, Xiao Z, et al. Novel coronavirus pneumonia outbreak in 2019: computed tomographic findings in two cases. *Korean J Radiol* 2020; 21(3):365-8. doi: 10.3348/kjr.2020.0078.
  10. Fang Y, Zhang H, Xie J, et al. Sensitivity of chest CT for COVID-19: comparison to RT-PCR. *Radiology* 2020; 296(2):E115-E7. doi: 10.1148/radiol.20200432.
  11. Pan F, Ye T, Sun P, et al. Time course of lung changes on chest CT during recovery from 2019 novel coronavirus (COVID-19) pneumonia. *Radiology* 2020; 295(3):715-21. doi: 10.1148/radiol.20200370.
  12. Duan YN, Qin J. Pre- and posttreatment chest CT findings: 2019 novel coronavirus (2019-nCoV) pneumonia. *Radiology* 2020; 295(1):21. doi: 10.1148/radiol.20200323.
  13. Fang X, Zhao M, Li S, et al. Changes of CT findings in a 2019 novel coronavirus (2019-nCoV) pneumonia patient. *QJM* 2020; 113(4):271-2. doi: 10.1093/qjmed/hcaa038.
  14. Shi H, Han X, Jiang N, et al. Radiological findings from 81 patients with COVID-19 pneumonia in Wuhan, China: a descriptive study. *Lancet Infect Dis* 2020; 20(4):425-34. doi: 10.1016/S1473-3099(20)30086-4.
  15. Ren LL, Wang YM, Wu ZQ, et al. Identification of a novel coronavirus causing severe pneumonia in human: a descriptive study. *Chin Med J (Engl)* 2020; 133(9):1015-24. doi: 10.1097/CM9.0000000000000722.
  16. Liu J, Zheng X, Tong Q, et al. Overlapping and discrete aspects of the pathology and pathogenesis of the emerging human pathogenic coronaviruses SARS-CoV, MERS-CoV, and 2019-nCoV. *J Med Virol* 2020; 92(5):491-4. doi: 10.1002/jmv.25709.
  17. Xu Z, Shi L, Wang Y, et al. Pathological findings of COVID-19 associated with acute respiratory distress syndrome. *Lancet Respir Med* 2020; 8(4):420-2. doi: 10.1016/S2213-2600(20)30076-X.
  18. Koo HJ, Lim S, Choe J, et al. Radiographic and CT features of viral pneumonia. *Radiographics* 2018; 38(3):719-39. doi: 10.1148/rg.2018170048.
  19. Chan MS, Chan IY, Fung KH, et al. High-resolution CT findings in patients with severe acute respiratory syndrome: a pattern-based approach. *AJR Am J Roentgenol* 2004; 182(1):49-56. doi: 10.2214/ajr.182.1.1820049.
  20. Hansell DM, Bankier AA, MacMahon H, et al. Fleischner Society: glossary of terms for thoracic imaging. *Radiology* 2008; 246(3):697-722. doi: 10.1148/radiol.2462070712.
  21. Ooi GC, Khong PL, Muller NL, et al. Severe acute respiratory syndrome: temporal lung changes at thin-section CT in 30 patients. *Radiology* 2004; 230(3):836-44. doi: 10.1148/radiol.2303030853.
  22. Das KM, Lee EY, Langer RD, et al. Middle East respiratory syndrome coronavirus: what does a radiologist need to know? *AJR Am J Roentgenol* 2016; 206(6):1193-201. doi: 10.2214/AJR.15.15363.
  23. Choi WJ, Lee KN, Kang EJ, et al. Middle East respiratory syndrome-coronavirus infection: a case report of serial computed tomographic findings in a young male patient. *Korean J Radiol* 2016; 17(1):166-70. doi: 10.3348/kjr.2016.17.1.166.
  24. Hamimi A. MERS-CoV: Middle East respiratory syndrome corona virus: can radiology be of help? Initial single center experience. *Egyptian J Radiol Nucl Med* 2015; 47(1):95-106. doi: 10.1016/j.ejrnm.2015.11.004.
  25. Das KM, Lee EY, Singh R, et al. Follow-up chest ra-

- diographic findings in patients with MERS-CoV after recovery. *Indian J Radiol Imaging* 2017; 27(3):342-9. doi: 10.4103/ijri.IJRI\_469\_16.
26. Zhao DW, Ma DQ, Wei W, et al. Early X-ray and CT appearances of severe acute respiratory syndrome an analysis of 28 cases. *Chin Med J* 2003; 116(6):823-6.
27. Goh SK, Tsou YY, Kaw JL. Severe acute respiratory syndrome (SARS): imaging findings during the acute and recovery phases of disease. *J Thorac Imaging* 2003; 18(3):195-9. doi: 10.1097/00005382-200307000-00010.
28. Nicolaou S, Al-Nakshabandi NA, Müller NL. SARS: imaging of severe acute respiratory syndrome. *AJR Am J Roentgenol* 2003; 180(5):1247-9. doi: 10.2214/ajr.180.5.1801247.
29. Wang R, Sun H, Song L, et al. Plain radiograph and CT features of 112 patients with SARS in acute stage. *Beijing Da Xue Xue Bao Yi Xue Ban* 2003; 35(Suppl):29-33.
30. Müller N, Ooi G, Khong P, et al. Severe acute respiratory syndrome: radiographic and CT findings. *AJR Am J Roentgenol* 2003; 181(1):3-8.
31. Zeng QS, Chen L, Hu WQ, et al. Roentgenography and CT appearance in patients with severe acute respiratory syndrome. *Zhonghua Jie He He Hu Xi Za Zhi* 2003; 26(6):347-49.
32. Müller NL, Ooi GC, Khong PL, et al. High-resolution CT findings of severe acute respiratory syndrome at presentation and after admission. *AJR Am J Roentgenol* 2004; 182(1):39-44. doi: 10.2214/ajr.182.1.1820039.
33. Chen H, Ai L, Lu H, et al. Clinical and imaging features of COVID-19. *Radiol Infect Dis* 2020; 27(2):43-50. doi: 10.1016/j.jrid.2020.04.003.
34. Kim EA, Lee KS, Primack SL, et al. Viral pneumonias in adults: radiologic and pathologic findings. *Radiographics* 2002; 22 Spec No:S137-49. doi: 10.1148/radiographics.22.suppl\_1.g02oc15s137..
35. Wang C, Horby PW, Hayden FG, et al. A novel coronavirus outbreak of global health concern. *Lancet* 2020; 395(10223):470-3. doi: 10.1016/S0140-6736(20)30185-9.
36. Li Y, Xia L. Coronavirus Disease 2019 (COVID-19): role of chest CT in diagnosis and management. *AJR Am J Roentgenol* 2020; 214(6):1280-6. doi: 10.2214/AJR.20.22954.
37. Wang CH, Liu CY, Wan YL, et al. Persistence of lung inflammation and lung cytokines with high-resolution CT abnormalities during recovery from SARS. *Respir Res* 2005; 6(1):42. doi: 10.1186/1465-9921-6-42.
38. Chang YC, Yu CJ, Chang SC, et al. Pulmonary sequelae in convalescent patients after severe acute respiratory syndrome: evaluation with thin-section CT. *Radiology* 2005; 236(3):1067-75. doi: 10.1148/radiol.2363040958.
39. Xie L, Liu Y, Xiao Y, et al. Follow-up study on pulmonary function and lung radiographic changes in rehabilitating severe acute respiratory syndrome patients after discharge. *Chest* 2005; 127(6):2119-24. doi: 10.1378/chest.127.6.2119.
40. Alsaad KO, Hajeer AH, Al BM, et al. Histopathology of Middle East respiratory syndrome coronavirus (MERS-CoV) infection—clinicopathological and ultrastructural study. *Histopathology* 2018; 72(3):516-24. doi: 10.1111/his.13379.